

# Micromachined 22 GHz PI filter by CMOS compatible ICP deep trench technology

T. Wang, Y.-S. Lin and S.-S. Lu

A K-band second-order bandpass filter with planar inductive  $\pi$ -network using CMOS technology is demonstrated for the first time. To reduce the substrate loss of the filter, the CMOS process compatible backside inductively-coupled-plasma (ICP) deep trench technology is used to selectively remove the silicon underneath the filter. After the ICP etching, a 55.5–92.2% improvement in quality factor is achieved for the inductors in the filter. In addition, a 1.1 dB improvement in maximum available power gain ( $G_{Amax}$ ) in K-band is achieved for the filter after the ICP etching. These results show that the micromachined  $\pi$  (PI) filter is very promising for microwave/millimetre-wave RFIC applications.

**Introduction:** Conventional second-order filters usually consist of two parallel resonators which are mutually coupled [1]. Since the mutual inductance (M) of the filters is usually very sensitive to the spacing between the two resonators, and the substrate thickness and material, tight control of the fabrication processes is necessary to meet the required specifications. Recently, it has been demonstrated that the bandwidth of a  $\pi$ -filter (i.e. a filter with the inductively-coupled  $\pi$ -network), either on a Teflon PCB board [2] or on a GaAs substrate [3], is quite insensitive to variation in the physical layout and substrate thickness, i.e. the  $\pi$ -filter exhibits larger design margin than the traditional one. In this work, for the first time, we implement a K-band  $\pi$ -filter by using a standard CMOS technology. To reduce loss, the post-ICP processing is used to selectively remove the silicon underneath the filter.

**Filter structure and ICP technology:** The filters were implemented in a 0.18  $\mu\text{m}$  CMOS technology. MIM capacitors and metal strips were used to realise the capacitances and inductances needed for the  $\pi$ -filter, respectively. Most of the structures were made of the top metal (M6) with thickness of 2  $\mu\text{m}$  aluminium. The front-side die photo of the fabricated filter is shown in Fig. 1a. After the devices were fabricated, post-ICP processing was performed on the backside of the die. The post-processing flow is shown in Fig. 1c. First, the photolithography was performed on the backside. Then, ICP was used to etch the open area from the backside. Finally, the photoresist on the backside was cleaned for test purpose. Fig. 1b shows the backside die photo of the filter. Clearly, the silicon underneath the filter is indeed nearly fully dry etched away since the front-side pattern can be seen from the backside.

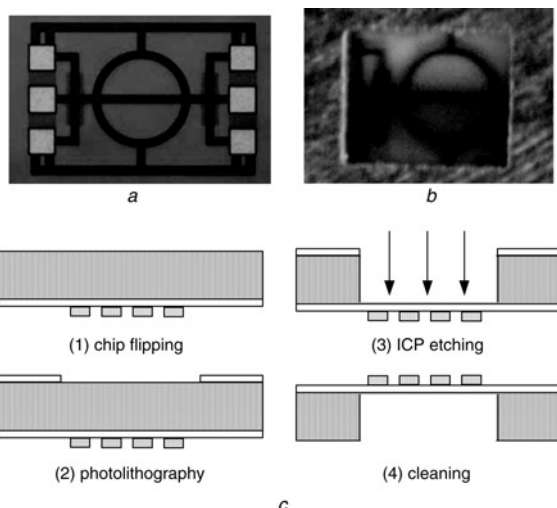


**Fig. 1** Front-side die photo (before ICP etching), backside die photo (after ICP etching) of the fabricated  $\pi$  (PI) filter, post-ICP processing flow  
 a Front-side  
 b Backside  
 c Post-ICP processing flow

**Principles of filter design:** The complete small-signal equivalent circuit model of the  $\pi$ -filters in Figs. 1a and b can be represented

by Fig. 2a. By using the delta-to-Y transformation [4], the circuit in Fig. 2a can be transformed to that shown in Fig. 2b, if the resistances in Fig. 2a are negligibly small. Suppose  $\alpha \equiv L_1/L_M$ , then we can show that  $L_A = L_1/(2 + \alpha)$  and  $L_B = L_M/(2 + \alpha)$ . Using the Y-to-delta transformation, the circuit in Fig. 2b can be transformed to that shown in Fig. 2c, in which LL and MM represent the parallel inductance of the resonators and the coupling inductance of the second-order bandpass filter proposed in [1], respectively. Based on the filter synthesis method introduced in [5], the values of  $C_e$ ,  $C_p$ , LL and MM in Fig. 2c can be determined based on the required specifications of ripple, centre frequency, and bandwidth. In addition, it can be shown that  $L_M$  and L in Fig. 2a can be represented as follows:

$$L_M = \frac{(2 + \alpha) \cdot LL^2}{2 \cdot LL + MM} - (2 + \alpha)L_{GND} \quad (1)$$

$$L = LL - L_M - 2 \cdot L_{GND} \quad (2)$$

For the 0.18  $\mu\text{m}$  CMOS technology adopted, the value of  $\alpha (\equiv L_1/L_M) \approx 4.19$ , which is nearly independent of the layout size of the  $\pi$ -filters. In addition,  $L_{GND}$  is specified as 2 pH. This means the values of L,  $L_1$  and  $L_M$  can be determined by (1) and (2) once the LL and MM values are known.

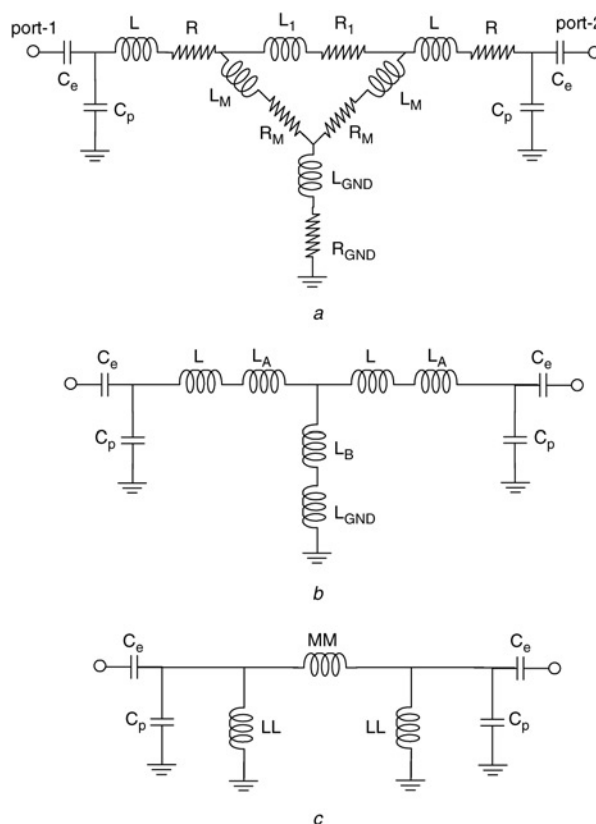


**Fig. 2** Complete, simplified, and further simplified equivalent lumped network of  $\pi$ -filters

a Complete  
 b Simplified  
 c Further simplified

**Measurement results and discussion:** The S-parameters of the filters were on-wafer measured from 2 to 40 GHz using a vector network analyser and a microwave probe station. After ICP etching, the power gain ( $S_{21}$ ) of the filter was slightly blue shifted owing to reduction of the substrate capacitance, and the peak value of  $S_{21}$  (at about 22 GHz) was improved by  $\sim 0.4$  dB owing to the elimination of substrate loss (not shown). Note that the reflection effect must be taken into account when the insertion losses of passive devices are compared. To exclude the effect of interfacial impedance mismatch, maximum available power gain ( $G_{Amax}$ ) is derived from the measured S-parameters according to [6] and shown in Fig. 3a. Clearly, the minimum power loss can be reduced by 1.1 dB in K-band (18–27 GHz) after substrate removal.

To gain more insights into the impacts of substrate removal, it is necessary to extract equivalent circuit parameters of the  $\pi$ -filters, before

and after backside ICP etching. The results show that all the simulated results were close to the measured data over the band of interest. Fig. 3b shows the measured and simulated results of the  $\pi$ -filter before ICP etching. The results are summarised in Table 1. As can be seen, the quality factors of the inductors in the filters were improved in a range from 55.5 to 92.2% after substrate removal. In addition to the quality factor improvement, the increased inductance and reduced capacitance imply that the metal strips without the underneath substrate become more inductive, which is more attractive for millimetre-wave circuits because inductance plays a more significant role in radio frequency such as tuned load, input matching, etc., and this ICP technique suggests a good method to eliminate the unwanted capacitive domination in the millimetre-wave range.

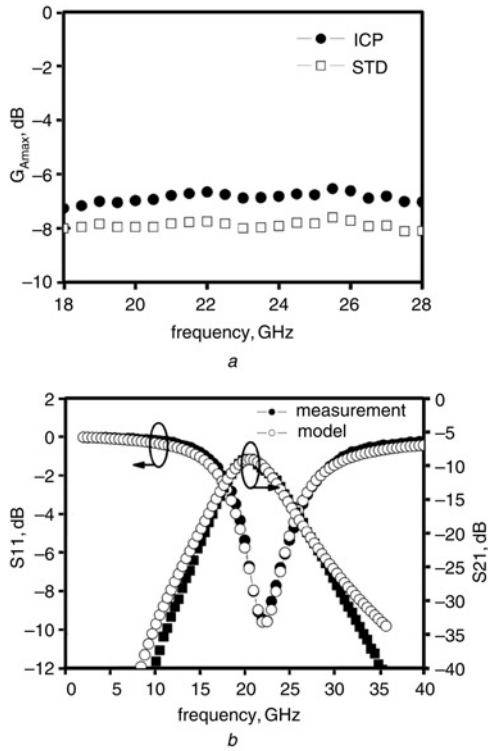


**Fig. 3** Measured  $G_{Amax}$  standard (STD) and post-IC processed (ICP) filters, and measured and simulated S-parameters of STD filter  
a Measured  $G_{Amax}$  of standard and post-IC processed (ICP) filter  
b Measured and simulated S-parameters of STD filter

**Table 1:** Extracted small-signal equivalent circuit parameters of  $\pi$ -filter both before and after ICP etching

	STD filter	ICP filter	Improvement
$L_1$ (pH)	201	207	
$L_M$ (pH)	48	48	
$L$ (pH)	63	64	
$L_{GND}$ (pH)	2	2	
$C_p$ (fF)	40	38.5	
$Q_{L1} (\equiv \omega L_1/R_1)$ at 22 GHz	7.7	14.8	92.2%
$Q_{LM} (\equiv \omega L_M/R_M)$ at 22 GHz	9	14	55.5%
$Q_L (\equiv \omega L/R)$ at 22 GHz	7.6	14	84.2%
$Q_{LGND} (\equiv \omega L_{GND}/R_{GND})$ at 22 GHz	7.8	14	79.5%

**Conclusion:** The CMOS compatible ICP deep trench technology is used to remove the silicon underneath a 22 GHz filter. Experimental results show that the  $G_{Amax}$  can be improved by 1.1 dB in K-band and the quality factors of the inductors in the filters are enhanced in a range from 55.5 to 92.2%.

© The Institution of Engineering and Technology 2007  
11 February 2007

Electronics Letters online no: 20070437  
doi: 10.1049/el:20070437

T. Wang and S.-S. Lu (Graduate Institute of Electronics Engineering and Department of Electrical Engineering, National Taiwan University, Taipei, Republic of China)

E-mail: sslu@ntu.edu.tw

Y.-S. Lin (Department of Electrical Engineering, National Chi Nan University, Puli, Republic of China)

#### References

- 1 Yeung, L.K., and Wu, K.L.: 'A compact second-order LTCC bandpass filter with two finite transmission zeros', *IEEE Trans. Microw. Theory Tech.*, 2003, **51**, (2), pp. 337–341
- 2 Lin, H.H., Tung, W.S., Cheng, J.C., and Chiang, Y.C.: 'Design of second order band-pass filter with inductive  $\pi$ -network coupling', *IEICE Trans. Commun.*, 2005, **E88-B**, (6), (2629–2631)
- 3 Tung, W.S., Chiu, H.C., and Chiang, Y.C.: 'Implementation of millimetre-wave bandpass filter with MMIC technology', *Electron. Lett.*, 2005, **41**, (13), pp. 744–745
- 4 Nilsson, J.W., and Riedel, S.A.: 'Electric circuits' (Prentice-Hall, New Jersey, 2002), pp. 433–434
- 5 Hung, J.S.G., and Lancaster, M.J.: 'Microstrip filters for RF/microwave applications' (Wiley-Interscience, 2001)
- 6 Ng, K.T., Rejaei, B., and Burghartz, J.N.: 'Substrate effects in monolithic RF transformers on silicon', *IEEE Trans. Microw. Theory Tech.*, 2002, **50**, (1), pp. 377–383